Diode Laser Assisted Surface Nitriding of Ti-6Al-4V: Properties of the Nitrided Surface

AMIT BISWAS, LIN LI, U.K. CHATTERJEE, I. MANNA,
and JYOTSNA DUTTA MAJUMDAR

In the present study, a detailed investigation of mechanical and electrochemical properties of laser-surface-nitrided Ti-6Al-4V has been carried out. Laser treatment is carried out by melting the surface of Ti-6Al-4V substrate using a high power CW diode laser with nitrogen as shrouding environment. The effect of laser parameters (applied power and gas flow rate) on the properties of the nitrided surface was evaluated. The microhardness of the nitrided surface was improved to a maximum of 1175 VHN in the present set of laser processing conditions as compared to 280 VHN of as-received substrate. Surface nitriding increased the potential for pit formation (E_{pit}) significantly as compared to as-received Ti-6Al-4V. Immersion in Hank's solution showed calcium phosphate deposition from the solution. The optimum process parameters for laser surface nitriding were derived.

DOI: 10.1007/s11661-009-0021-0

I. INTRODUCTION

TITANIUM and its alloys are widely used as surgical implants.[1] However, poor wear resistance and loss of adhesion at the interface cause restriction over prolonged use of the component especially as implants for hip joints and teeth.[2] Important surface characteristics, which can contribute to a strong interfacial joint, are (1) the existence of polar chemical groups or coupling agents on the surfaces that are available for bonding; and (2) increased surface roughness, giving rise to improved mechanical interlocking or increased bondable surface area.[3] Over the last decade, various types of surface modification techniques have been developed aiming at improving the interfacial bonding of the alloy with the bone and improving wear resistance.[4–7] Laser as a source of monochromatic and coherent radiation has wide ranging applications in surface treatment.[8,9] Laser surface remelting of titanium in the nitrogen containing environment is popularly known as laser gas nitriding, which can produce composite surface layers consisting of nitrides with enhanced surface performance.[10,11] The advantages of laser assisted surface treatment over conventional diffusion-aided surface treatment include the ability to deliver a large power/energy density (10^3 to 10^5 W/cm^2), high heating/cooling rate (10^3 to 10^5 K/s), and solidification velocities (1 to 30 m/s).[8,9]

Laser gas nitriding of Ti and Ti-6Al-4V (Ti64) alloys has been extensively investigated with the aim of improving the tribological properties.[10,12–14] It was observed that a complex microstructure is developed in the solidified melt pool depending on the applied laser power, beam size, specimen velocity, beam mode (stationary or spinning), and nitrogen concentration in the environment.[15] Furthermore, cracking was found to be a critical problem in laser surface nitriding of titanium alloys due to a large residual stress developed in the nitrided zone.[16] Man *et al.*[17] nitrided the surface of the Ti-6Al-4V substrate using a CW Nd:YAG laser and carried out a detailed X-ray photoelectron spectroscopic (XPS) observation, comparing it with the results after mechanical polishing. A very thin oxide layer was detected on the near-surface region, which decreased with increasing depth.

Since the report on application of diode laser in materials processing, it has become increasingly popular in different fields of materials processing such as cutting, welding, and direct laser cladding.[18] In an earlier study, diode laser assisted surface nitriding of Ti-6Al-4V was attempted and showed an improvement in hardness and biocompatibility.[19] In the present study, a detailed investigation of the influence of laser parameters on the mechanical and electrochemical properties of the surface-nitrided layer has been undertaken. Finally, the optimum process parameters for laser surface nitriding of Ti-6Al-4V have been determined following a detailed structure-property-process parameters correlation.

II. EXPERIMENTAL

In the present investigation, Ti-6Al-4V (Ti64) of dimensions 20 mm × 20 mm × 5 mm was chosen as the substrate. The substrate surface was sand blasted prior to laser processing in order to clean the surface and

AMIT BISWAS, Lecturer, U.K. CHATTERJEE and I. MANNA, Professors, and JYOTSNA DUTTA MAJUMDAR, Associate Professor, are with the Department of Metallurgy and Materials Engineering, IIT, Kharagpur, W.B.-721302, India. Contact e-mail: jyotsna@metal.iitkgp.ernet.in LIN LI, Professor, is with the School of Mechanical Aerospace and Civil Engineering, University of Manchester, Manchester, M60 1QD, United Kingdom.

Manuscript submitted August 1, 2008.
Article published online October 9, 2009

improve absorptivity. Laser surface nitriding was carried out by irradiating the substrate using a 2 kW continuous wave (CW) Laserline diode laser with mixed 810- and 940-nm wavelengths (maximum power of 1.5 kW) and with an optical fiber beam delivery system (with a spot area of 3.5 × 2 mm^2) using nitrogen as the shrouding gas. The main process variables used in the present study were applied laser power and gas flow rate. The range of power used in the present study was from 600 to 800 W; the range of gas flow rate was from 5 to 20 L/min. The scan speed was maintained constant at 6 mm/s. Table I summarizes the process parameters and properties of the as-received *vis-à-vis* laser-surface-nitrided Ti-6Al-4V as a function of laser parameters. To achieve microstructural and compositional homogeneity of the laser-treated surface, a 25 pct overlap between the successive melt tracks was followed. To ensure rapid cooling, N_2 gas flow was maintained at 20 L/min, following each melting track for 1 minute. Following laser surface nitriding, the microstructure of the nitrided layer (both the top surface and the cross section) was characterized by optical and scanning electron microscopy. In this regard, it is relevant to mention that the approximate surface roughness of laser-surface-nitrided samples as measured by the mechanical profilometer (diamond stylus) was 10 to 15 μm. A detailed analysis of the phase was carried out using an X-ray diffractometer. Residual stress introduced in the nitrided layer was measured by a stress goniometer attached to an X-ray diffractometer applying Cohen's theory.[20] The microhardness of the nitrided layer (both the top surface and cross-sectional plane) was measured by a Vickers microhardness tester using a 300 g applied load. The Young's modulus and its distribution were evaluated with the help of a MTS-XP nanoindenter (MTS Systems Co., Nano Instruments, Oak Ridge, TN). The indentation was conducted by application of a triangular pyramid (Berkovich, MTS Systems Co., Nano Instruments, Oak Ridge, TN) diamond indenter with an applied load varying from 100 to 500 mN. During the measurement, 50 to 100 readings were recorded at a particular load to take the average value of a particular region. The electrochemical property of the surface in terms of pitting corrosion resistance was compared to that of the as-received Ti-6Al-4V by potentiodynamic anodic polarization study in Hank's solution with the following electrolytic composition (g/L): 0.185$CaCl_2$, 0.4KCl, 0.06KH_2PO_4, 0.1$MgCl_2$, 6H_2O, 0.1$MgSO_4 \cdot 7H_2O$, 8NaCl, 0.35$NaHCO_3$, 0.48Na_2HPO_4, and 1.00 D-glucose. In the corrosion study, a standard calomel electrode was used as the reference electrode and platinum was used as the counterelectrode.[21] Polarization was carried out from −2000 to + 7000 mV (SCE) at a scan rate of 2 mV/s. The pitting corrosion behavior was determined by measuring the primary potential for pit formation, E_{pp1} (the potential at which there is a sudden rise in current density with a small increase in potential). The samples (as-received and laser surface treated) under polished conditions were immersed in Hank's solution, and the corroded surface was carefully examined (at a regular interval) using a scanning electron microscope to understand the extent of corrosion. Subsequently, the phases present on the corroded surface were also examined by the X-ray diffraction technique.

The wettability of the simulated body fluid (SBF) on the surface of the as-received and thermally oxidized AZ91 was evaluated using the sessile-drop technique.[22] During the measurement, a drop (of diameter 0.5 to 1 mm) of SBF was released from the tip of a syringe onto a sample surface, and the contact angle the drop made with the surface was measured by taking a digital image of the drop. The accuracy of the contact angle measurements was within ±1 deg.

Table I. Summary of Laser Parameters for Laser Surface Nitriding of Ti-6Al-4V and Mechanical and Electrochemical Properties of the Melt Zone

Applied Power, W (Gas Flow Rate, L/min)	Microhardness (VHN)	Young's Modulus (GPa)	Critical Potential for Pit Formation V(SCE)
600(5)	892	170	6.0
600(10)	1142	177	5.2
600(20)	780	178	2.5
700(5)	912	171	1.8
700(10)	1075	175	1.2
700(20)	632	177	1.6
800(5)	897	173	1.4
800(10)	1102	177	1.7
800(20)	783	175	1.8
As-received Ti-6Al-4V	280	115	1.3

III. RESULTS AND DISCUSSION

In the present investigation, a detailed study of the mechanical (microhardness) and electrochemical (corrosion resistance) properties of the surface-nitrided layer was undertaken and compared with a study of the as-received Ti-6Al-4V substrate. The results of the mechanical and electrochemical properties of the nitrided layer are discussed in detail.

A. *Characteristics of the Nitrided Zone*

Figure 1 shows the scanning electron micrograph of the top surface of laser-surface-nitrided Ti-6Al-4V lased

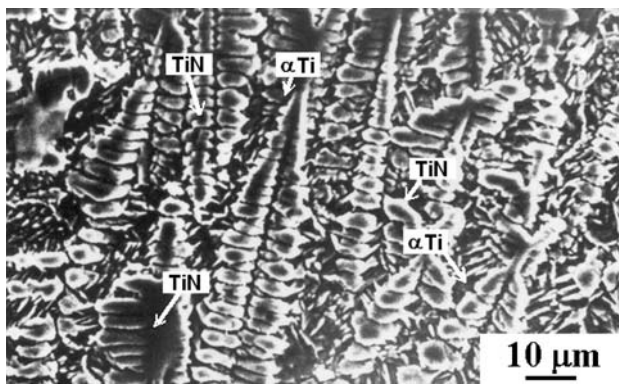

Fig. 1—Scanning electron micrograph of the top surface of laser-surface-nitrided Ti-6Al-4V lased with power of 600 W and gas flow rate of 10 L/min.

with a power of 600 W, scan speed of 6 mm/s, and gas flow rate of 10 L/min. From Figure 1, it may be noted that laser surface nitriding causes formation of a continuous and defect-free (microporosity and microcrack) nitride surface. The nitrided layer consists of dendrites of titanium nitride in a α-Ti matrix (as confirmed by X-ray diffraction analysis) with an average interdendritic spacing of 2 to 4 μm (between TiN and TiN) for different conditions of lasing. Average surface roughness measured by atomic force microscopy from the surface topography of the diamond polished surface was found to increase from 0.040 μm in as-received to 0.29 μm for laser-surface-nitrided and subsequently diamond-polished Ti-6Al-4V.[23] A rough surface was reported to cause more adsorption offibronectin, a cell adhesion protein present in serum, which mediates cell attachment and spread on artificial substrates by interacting with glycosaminoglycans and the cytoskeleton,[24] than smooth surfaces,[25] preserving the synthesis of extracellular matrix proteins.[26] Culturing rat calvarial cells on titanium surfaces in a range of surface roughness (R_a) from 0.14 to 1.15 μm has shown a maximum attachment on the surfaces with a surface roughness (R_a) of 0.87 μm.[27] Hence, the increase in surface roughness level following laser surface nitriding would be beneficial for improved biocompatibility.

A detailed X-ray diffraction analysis of the top surface of as-received and laser-surface-nitrided Ti-6Al-4V was undertaken to understand the phases present and quantify their volume fraction. Figure 2 compares the X-ray diffraction profiles of the surface of as-received (plot 1) with laser-surface-nitrided Ti-6Al-4V (plot 2) lased with a power of 600 W and gas flow rate of 10 L/min. From the X-ray diffraction profiles, it is shown that as-received Ti-6Al-4V used in the present study consists of a mixture of α and β titanium. Laser surface nitriding of Ti-6Al-4V led to the formation of TiN and a few α-Ti. The mass fraction of titanium nitride dendrite was found to vary with laser parameters. The residual stress developed in the nitrided zone was measured by the X-ray diffraction technique using a stress goniometer. The residual stress developed on the top surface of the nitrided samples was found to vary significantly (+750 to −1400 MPa) with laser parameters. It was observed that residual stress was compressive only when lased with a higher applied power (800 W). A decrease in gas flow rate was found to increase the magnitude of compressive stress within the surface.

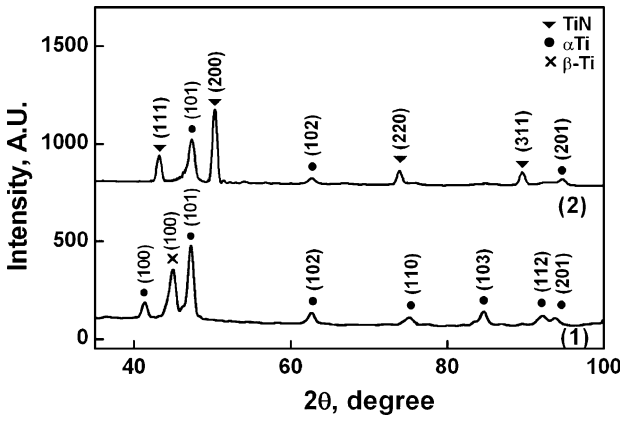

Fig. 2—X-ray diffraction profiles of as-received (plot 1) and laser-surface-nitrided Ti-6Al-4V lased with power of 600 W and gas flow rate of 10 L/min.

B. *Mechanical Properties of the Nitrided Surface*

Figures 3(a) and (b) show the variation of microhardness along the cross-sectional plane with depth from the surface of laser-surface-nitrided Ti-6Al-4V. Figure 3(a) shows the microhardness profiles of laser-surface-nitrided Ti-6Al-4V lased with power of 600 W (plot 1), 700 W (plot 2), and (3) 800 W (plot 3) at a nitrogen gas flow rate of 10 L/min. Figure 3(b) shows the microhardness profiles of the nitrided zone lased

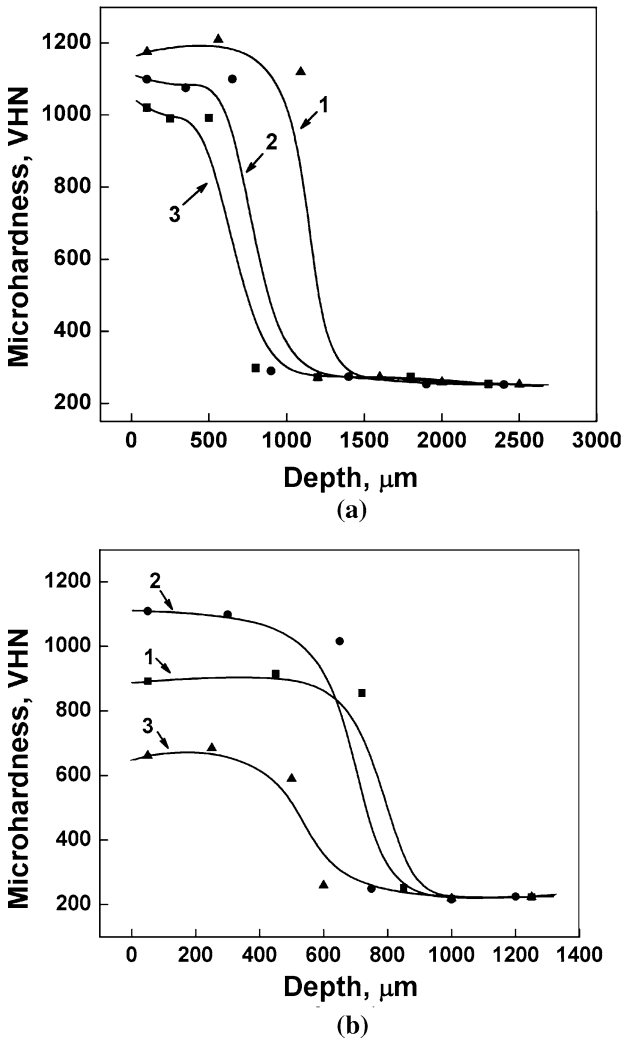

Fig. 3—Variation of microhardness with depth from the surface of laser-surface-nitrided Tii-6Al-4V showing the effect of (*a*) applied power lased at a nitrogen gas flow rate of 10 L/min and power of 600 W (plot 1), 700 W (plot 2), and (3) 800 W (plot 3), and (b) nitrogen gas flow rate lased at an applied power of 700 W and gas flow rate of 5 L/min (plot 1), 10 L/min (plot 2), and 20 L/min (plot 3).

with an applied power of 700 W and at a gas flow rate of 5 L/min (plot 1), 10 L/min (plot 2), and 20 L/min (plot 3). The high hardness confined to the near-surface region corresponds to the nitride zone. From Figures 3(a) and (b), it is evident that the microhardness in the nitrided zone is significantly improved and is almost uniform reaching the substrate microhardness (280 VHN) along the nitride zone–substrate interface. Furthermore, the average microhardness of the nitrided layer decreases with the increase in laser power (*cf.* Figure 3(a)). The decreased microhardness with the increase in applied power is due to coarsening of the microstructure. From Figure 3(b), it is clear that the microhardness of the nitrided layer increases with an increase in gas flow rate from 5 to 10 L/min (plot 1 *vs* plot 2) and then decreases (plot 3) with an increase in gas flow rate to 20 L/min. Maximum surface hardness was developed when the laser surface nitrided with an applied power of 600 W and gas flow rate of 10 L/min (1175 VHN), which is over 4 times higher than the base hardness (280 VHN). Hence, it may be concluded that the mechanism of hardening in laser-surface-nitrided Ti-6Al-4V is because of the formation of nitrides and refinement of microstructures.

Nanoindentation tests were conducted by means of a MTS-XP nanoindenter to evaluate the hardness and elastic modulus distribution in the localized region of the treated surface. The indentation was conducted by application of a triangular pyramid (Berkovich) diamond indenter with an applied load varying from 100 to 500 Mn. Test works 4 software (MTS Systems Co., Nano Instruments, Oak Ridge, TN) for the nanoindentation system was used to calculate the hardness and Young's modulus from a load-displacement graph using the Oliver and Pharr method.[28] During the measurement, 50 to 100 readings were recorded at a particular load to take the average value of a particular region. Hence, the Young's modulus reported in the present study is the average of α-Ti and TiN.

Table I summarizes the average Young's modulus of the as-received and surface-nitrided Ti-6Al-4V under all processing conditions. From Table I, it may be noted that the Young's modulus of the nitrided surface is significantly improved (171 to 175 GPa) as compared to the as-received Ti-6Al-4V (115 GPa).

C. *Electrochemical Properties of the Nitrided Surface*

Figure 4 presents the bar chart comparing the measured potential for pit formation (E_{pp1}) of as-received *vis-à-vis* laser-surface-nitrided Ti-6Al-4V for different laser parameters, and the corresponding quantitative data are presented in Table I. It is interesting to note that the measured pitting potential (E_{pp1}) of the nitrided surface (in Hank's solution) does not deteriorate and is nobler in all the samples processed under the present set of parameters. Furthermore, E_{pp1} increases significantly as compared to as-received Ti-6Al-4V under two different sets of parameters. Careful observation of Figure 4 and Table I shows that E_{PP1} decreases with the increase in applied power. On the other hand, the E_{PP1} of the nitrided surface decreases with the increase in nitrogen

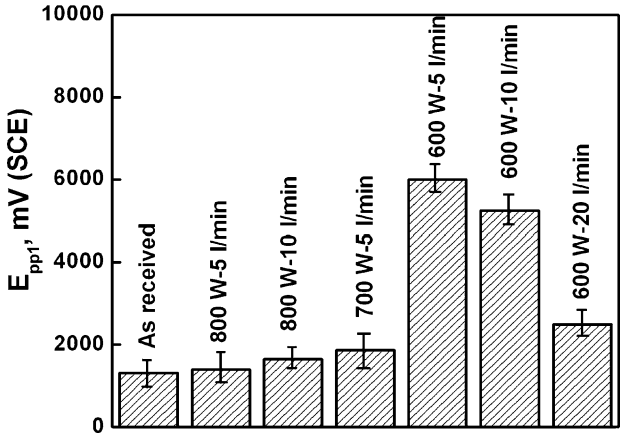

Fig. 4—Bar charts showing the variation of critical potential for pit formation (E_{PP1}) with laser parameters.

gas flow rate at 600 W but not at 800 W. Increased pitting potential due to surface nitriding is due to the presence of TiN on the surface and the presence of nitrogen in solution. The presence of the surface roughness, on the other hand, deteriorates the pitting corrosion property. Increasing power was found to coarsen the microstructure and increase the surface roughness (*cf.* Table II), which is possibly responsible for decreasing the E_{PP1} at a higher power level. On the other hand, increasing the gas flow rate leads to the formation of fragmented dendrites and, hence, the presence of a large number of interfaces and a reduced mass fraction of titanium nitride in the alloyed zone; as a result, E_{PP1} is reduced at a higher nitrogen flow rate.

A detailed study of the corroded surface formed on as-received and laser-surface-nitrided Ti-6Al-4V was undertaken to understand the genesis of corrosion. Figures 5(a) and (b) show the detailed X-ray diffraction profiles of the corroded film formed on (a) as-received and (b) laser-surface-nitrided (with a power of 600 W and nitrogen gas flow of 10 L/min) Ti-6Al-4V followed by immersion in Hank's solution for 72 hours. From the X-ray diffraction profile, it is relevant that TiO_2 is the main constituent of the oxide scale formed on as-received and laser-surface-nitrided Ti-6Al-4V samples. The presence of $Ca_3(PO_4)_2$ peaks was also found to be present on the corroded film of both surfaces. In the laser-surface-nitrided sample, the presence of TiN peaks was also observed. The presence of nitrogen in the solution and nitrides were both responsible for improving the pitting corrosion property of the surface-nitrided Ti-6Al-4V samples. Figures 6(a) and (b) show the microstructures of corroded films formed on (a) as-received and (b) laser-surface-nitrided (with a power of 600 W and nitrogen gas flow of 10 L/min) Ti-6Al-4V followed by immersion in Hank's solution for 72 hours. From Figures 6(a) and (b), it is relevant that the microstructure of the corroded surface mainly consists of localized pitted regions. In the as-received Ti-6Al-4V, the area fraction of the pit is significantly higher than the laser-surface-nitrided samples, suggesting the interconnection of pits for a longer duration for both samples tested for 72 hours. Very finely distributed calcium

Table II. Summary of Optimum Laser Parameters for Laser Surface Nitriding of Ti-6Al4V and Properties of the Nitrided Zone

Applied Power, W (Gas Flow Rate, L/min)	Microhardness (VHN)	Residual Stress (MPa)	Young's Modulus (GPa)	Contact Angle	Critical Potential for Pit Formation V(SCE)
700(5)	912	−50	171	45 ± 1 deg	1.8
800(5)	897	−2450	173	41 ± 1 deg	1.4
800(10)	1102	−1250	177	48 ± 1 deg	1.7
800(20)	783	−1250	175	43 ± 1 deg	1.8
As-received Ti-6Al-4V	280	50	115	60 ± 1 deg	1.3

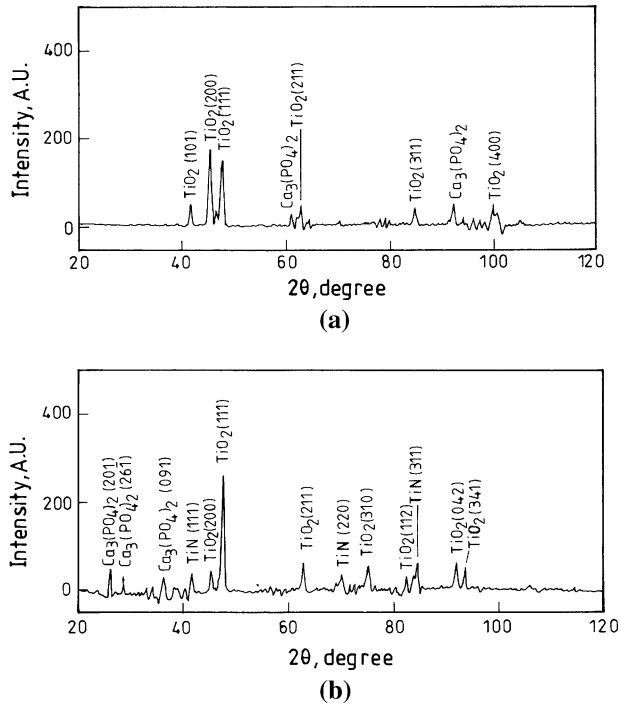

Fig. 5—X-ray diffraction profiles of (*a*) as-received and (*b*) laser-surface-nitrided (lased with a power of 600 W and nitrogen gas flow of 10 L/min) Ti-6Al-4V followed by immersion in Hank's solution for 72 h.

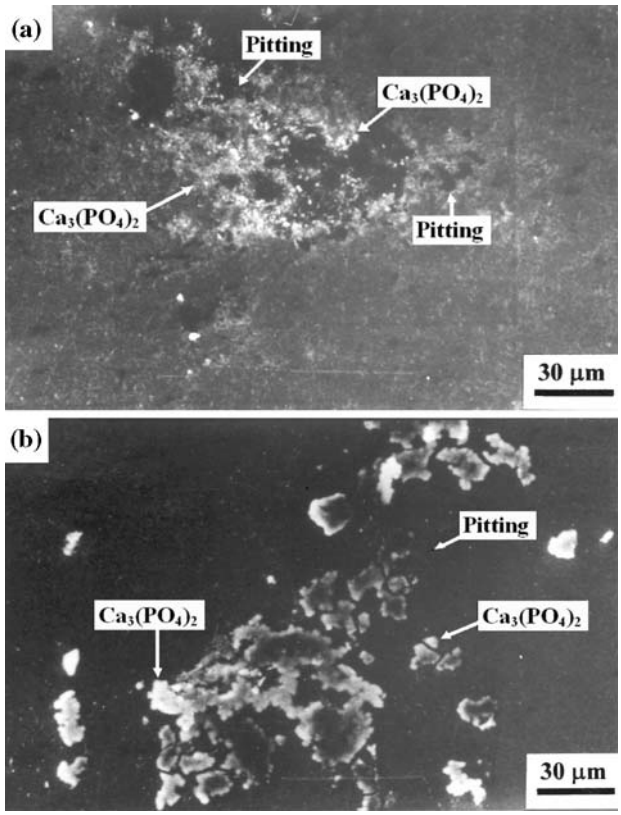

Fig. 6—Scanning electron micrograph of the top surface of (*a*) as-received and (*b*) laser-surface-nitrided (lased with a power of 600 W and nitrogen gas flow of 10 L/min) Ti-6Al-4V followed by immersion in Hank's solution for 72 h.

phosphate ($Ca_3(PO_4)_2$) was found to be present in the microstructure. A close comparison between Figures 6(a) and (b) reveals that the area fraction of pits is reduced by nitriding with an increase in the amount of $Ca_3(PO_4)_2$ phase in the microstructure. $Ca_3(PO_4)_2$ makes the implant surface more active for osteointegration; it enhances bone attachment with the implant and also makes the surface more compatible for bone ingrowth.

D. *Wettability Behavior*

Table II shows the variation of contact angle of a SBF droplet on as-received and laser-surface-nitrided Ti-6Al-4V surface under optimum laser parameters (*cf.* Table II). The as-received sample has an angle of contact of 60 deg. On the nitrided surface, the contact angle of SBF is reduced to 41 to 48 deg. From Table II, it is evident that the variation of contact angle with laser parameters does not show any specific trend. The decrease in contact angle of the droplets on the nitrided surface as compared to the as-received Ti-6Al-4V is attributed to the change in surface composition and increase in surface roughness due to nitriding. It is well known that hydroperoxide or other polar groups generated from oxidation causes the water contact angle to decrease and increase in hydrophilicity. The changing of the contact angle of the nitrided surface implied that the surface was more wettable against SBF. Cell adhesion is generally better on hydrophilic surfaces.[29]

IV. PROCESS OPTIMIZATION

A detailed correlation between the mechanical and electrochemical properties and process parameters (laser power and gas flow rate) was undertaken to optimize the

process parameters for laser surface nitriding of Ti-6Al-4V in the present study. Table I summarizes the properties of the as-received *vis-à-vis* laser-surface-nitrided Ti-6Al-4V as a function of laser parameters. In the present study, laser surface nitriding was conducted with an applied power ranging from 600 to 800 W and a gas flow rate ranging from 5 to 20 L/min. Application of too low a power was unable to melt the surface or too high power caused surface evaporation. On the other hand, application of a too high gas flow rate increased the surface roughness and microdefect formation. Too low a gas flow rate caused oxidation of the surface. Laser surface nitriding under the present set of laser parameters ensured formation of a defect-free (microporosity and microcrack) and homogeneous microstructure. The microhardness of the nitrided surface is significantly improved to 632 to 1075 VHN as compared to the 280 VHN of the as-received substrate, though its magnitude was found to decrease with the increase in applied power, and a maximum microhardness value was achieved at an applied power of 600 W and a gas flow rate of 10 L/min. However, introduction of residual stress is a problem associated with laser surface nitriding. As compressive residual stress is beneficial for the surface fatigue property and tensile stress is detrimental, optimum selection of laser parameters is essential to ensure compressive residual stress. It was observed that residual stress was compressive only when lased with a higher applied power (800 W). A decrease in gas flow rate was found to increase the magnitude of compressive stress within the surface. Improvement in pitting corrosion resistance in Hank's solution was observed in the nitrided surface under the present set of laser parameters, though the improvement in pitting potential is significant when lased with an applied laser power of 600 W and nitrogen gas flow rate of 5 and 10 L/min. From the correlation of laser parameters with microstructures, residual stress, improvement of microhardness, pitting corrosion resistance (E_{pp1}), uniform corrosion resistance (E_{corr}), and enhanced wettability (which is required for improved cell adherence), the optimum combinations of laser parameters derived from the present study are tabulated in Table II.

V. SUMMARY AND CONCLUSIONS

In the present investigation, a detailed study of the mechanical and electrochemical properties of laser-surface-nitrided Ti-6Al-4V has been carried out. From the detailed analysis, the following conclusions can be drawn.

1. Laser surface nitriding leads to formation of a defect-free (microporosity and microcrack) nitride zone with the presence of TiN dendrites in the α-Ti matrix. The mass fraction of nitride (40 to 95 pct) varied with laser parameters. An increased surface roughness was noticed on the nitrided surface.
2. The microhardness of the nitrided zone is significantly increased to 600 to 1200 VHN as compared to 280 VHN of as-received Ti-6Al-4V substrate. Microhardness of the nitrided surface decreases with the increase in applied power. The increase in gas flow rate initially increases the microhardness of the nitride layer; however, at a too high gas flow rate, the microhardness decreases.
3. The average bulk modulus of the nitrided layer was increased to 171 to 177 GPA as compared to 114 GPA of the as-received Ti-6Al-4V.
4. A significant improvement in pitting corrosion resistance was achieved by laser surface nitriding in terms of critical potential for pit formation only for an applied laser power of 600 W and nitrogen gas flow of 5 and 10 L/min. Calcium phosphate deposition was found in both the surfaces following dipping in a SBF, though the extent was higher in the nitrided surface.
5. Wettability of the nitrided surface against SBF was significantly increased as compared to as-received Ti-6Al-4V.

ACKNOWLEDGMENTS

The financial support for this work from the Council of Scientific and Industrial Research (CSIR, N. Delhi) and the Board of Research on Nuclear Science (BRNS, Bombay) is gratefully acknowledged.

REFERENCES

1. *Titanium and Titanium Alloys*, M.J. Donachie, Jr., ed., ASM, Metals Park, OH, 1982, p. 3.
2. E.I. Meletis, C.V. Cooper, and K. Marchev: *Surf. Coat. Technol.*, 1999, vol. 113, pp. 201–09.
3. R.R. Wang, G.E. Welsch, and O. Monteiro: *J. Biomed. Mater. Res.*, 1999, vol. 46, pp. 262–70.
4. M.C. Kuo and S.K. Yen: *Mater. Sci. Eng. C*, 2002, vol. 20, pp. 153–60.
5. W. Shi, A. Kamiya, J. Zhu, and A. Watazu: *Mater. Sci. Eng. A*, 2002, vol. 337, pp. 104–09.
6. E.S. Thian, K.A. Khor, N.H. Loh, and S.B. Tor: *Biomaterials*, 2001, vol. 22, pp. 1225–32.
7. A.K. Lynn and D.L. DuQuesnay: *Biomaterials*, 2002, vol. 23, pp. 1937–46.
8. J. Dutta Majumdar and I. Manna: *Sadhana*, 2003, vol. 28, pp. 495–562.
9. B.L. Mordike: in *Laser Surface Treatment of Metal*, C.W. Draper and P. Mazzoldio, eds., Martinus Nijhoff, Dordrecht, 1986, pp. 389–413.
10. B.L. Mordike: *Prog. Mater. Sci.*, 1997, vol. 42, pp. 357–72.
11. I. Bertoti, M. Mohai, J.L. Sullivan, and S.O. Saied: *Appl. Surf. Sci.*, 1995, vol. 84, pp. 357–72.
12. T. Bell, H.W. Bergmann, J. Lanagan, P.H. Morton, and A.M. Staines: *J. Surf. Eng.*, 1986, vol. 2, pp. 133–43.
13. A. Walker, J. Folkes, W.M. Steen, and D.R.F. West: *J. Surf. Eng.*, 1986, vol. 1, pp. 133–43.
14. S. Mridha and T.N. Baker: *Mater. Sci. Eng. A*, 1994, vol. 188, pp. 229–39.
15. C. Hu, H. Xin, L.M. Watson, and T.N. Baker: *Acta Mater.*, 1997, vol. 45, pp. 4311–22.
16. J.M. Robinson, B.A. Van Brussel, J.T.M. De Hosson, and R.C. Reed: *J. Mater. Sci. A*, 1996, vol. 208, pp. 143–47.
17. H.C. Man, Z.D. Cui, and X.J. Yang: *Appl. Surf. Sci.*, 2002, vol. 199, pp. 293–302.
18. L. Li: *Opt. Las. Eng.*, 2000, vol. 34, pp. 231–53.
19. A. Biswas, L. Li, T.K. Maity, U.K. Chatterjee, I. Manna, B.L. Mordike, and J. Dutta Majumdar: *Las. Eng.*, 2007, vol. 16, pp. 434–38.

20. B.D. Cullity and S.R. Stock: *Elements of X-Ray Diffraction*, 3rd ed., Prentice Hall, N. Delhi, 2001, p. 435.
21. M.G. Fontana: *Corr. Eng.*, McGraw-Hill, New York, NY, 1987, p. 71.
22. W. Adamson: *Phys. Chem. Surf.*, John Wiley, New York, NY, 1990, p. 298.
23. A. Biswas, L. Li, U.K. Chatterjee, I. Manna, S.K. Pabi, and J. Dutta Majumdar: *Scripta Mater.*, 2008, vol. 59, pp. 239–42.
24. B.S. Pearson, R.J. Klebe, B.D. Boyan, and D. Moskowicz: *J. Dent. Res.*, 1988, vol. 67, pp. 515–17.
25. R.E. Weiss and A.H. Reddi: *J. Cell. Biol.*, 1981, vol. 88, pp. 630–36.
26. J.Y. Martin, Z. Schwartz, T.W. Hummert, D.M. Schraub, J. Simpson, J. Lankford, D.D. Dean, D.L. Cochran, and B.D. Boyan: *J. Biomed. Mater. Res.*, 1995, vol. 29, pp. 389–401.
27. K.T. Bowers, J.C. Keller, B.A. Randolph, D.G. Wick, and C.M. Michaels: *Int. J. Oral Maxillofac. Implants*, 1992, vol. 7, pp. 302–10.
28. W.C. Oliver and G.M. Pharr: *J. Mater. Res.*, 1992, vol. 7, pp. 1564–83.
29. X. Zhu, J. Chen, L. Scheideler, R. Reichl, and J. Geis-Gerstorfer: *Biomaterials*, 2004, vol. 25, pp. 4087–4103.